Journal of ELECTRONIC MATERIALS, Vol. 40, No. 6, 2011
DOI: 10.1007/s11664-011-1518-z

Stabilization of the Thermal Decomposition of Poly(Propylene Carbonate) Through Copper Ion Incorporation and Use in Self-Patterning

TODD J. SPENCER,[1] YU-CHUN CHEN,[1] RAJARSHI SAHA,[1] and PAUL A. KOHL[1,2]

1.—School of Chemical and Biomolecular Engineering, Georgia Institute of Technology, Atlanta, GA 30332-0100, USA. 2.—e-mail: paul.kohl@chbe.gatech.edu

Incorporation of copper ions into poly(propylene carbonate) (PPC) films cast from γ-butyrolactone (GBL), trichloroethylene (TCE) or methylene chloride (MeCl) solutions containing a photo-acid generator is shown to stabilize the PPC from thermal decomposition. Copper ions were introduced into the PPC mixtures by bringing the polymer mixture into contact with copper metal. The metal was oxidized and dissolved into the PPC mixture. The dissolved copper interferes with the decomposition mechanism of PPC, raising its decomposition temperature. Thermogravimetric analysis shows that copper ions make PPC more stable by up to 50°C. Spectroscopic analysis indicates that copper ions may stabilize terminal carboxylic acid groups, inhibiting PPC decomposition. The change in thermal stability based on PPC exposure to patterned copper substrates was used to provide a self-aligned patterning method for PPC on copper traces without the need for an additional photopatterning registration step. Thermal decomposition of PPC is then used to create air isolation regions around the copper traces. The spatial resolution of the self-patterning PPC process is limited by the lateral diffusion of the copper ions within the PPC. The concentration profiles of copper within the PPC, patterning resolution, and temperature effects on the PPC decomposition have been studied.

Key words: Sacrificial material, polymers, air cavity

INTRODUCTION

Air cavities are of interest in microelectronic packages and microelectromechanical systems (MEMS) for microfluidic devices,[1–4] cantilever resonators,[5] and electrical insulation.[6] Air-cavity encapsulation of copper signal lines is particularly valuable because it increases the signal-to-noise ratio in copper connections, increases the electric field propagation velocity, and enables high-frequency signaling while consuming less energy per bit transmitted. Methods of producing low-loss, air-cavity insulation which use self-aligned, simple processing techniques are especially valuable.

Sacrificial materials patterned in precisely defined geometries can be used to create air-cavity encapsulation of components, such as electrical signal wires. Poly(propylene carbonate) (PPC) has been used as a sacrificial placeholder to define air-cavity regions around electrical signal wires.[1,5–7] The PPC was overcoated with a dielectric material, then thermally decomposed into gaseous products with low molecular weight, which permeate through the overcoat layer, leaving a precise air cavity.[3,7–9] Alternating layers of conductors and insulators can be fabricated to create air insulation, however each layer of PPC requires a photolithographic step in addition to patterning of the line and via-hole

(Received July 20, 2010; accepted January 7, 2011; published online March 3, 2011)

connections. Copper conductors are of the most interest because they have high conductivity and are of low cost. Thus, air encapsulation of copper conductors is of most interest.

PPC is a copolymer of carbon dioxide and propylene oxide, polymerized at high pressure in the presence of catalyst.[10–18] High-purity forms of the polymer exist in highly regular alternating units without including ether linkages in the backbone. Local variations in backbone structure exist, as shown in Fig. 1, known as head-to-head (HH), head-to-tail (HT), and tail-to-tail (TT). The pure, highly regular form of PPC (HT) has the highest glass-transition temperature, highest modulus, and highest decomposition temperature, because longer-chain polymers have fewer terminations where decomposition can initiate. PPC decomposes by chain scission and unzipping.[11,19–21] Decomposition propagates via chain unzipping at low temperatures because the cyclic monomer is thermodynamically more favored than the straight chain polymer. At higher temperatures, chain scission competes with the unzipping decomposition mechanism. Acid activation lowers the decomposition temperature by destabilizing the polymer and promoting ring cyclization into the monomer. This decomposition process is summarized in Fig. 2. An acid is regenerated after each cyclic monomer detaches from the backbone, propagating decomposition rapidly near room temperature. Heating on a hotplate is required to volatilize products, primarily cyclic propylene carbonate, acetone, carbon dioxide, and low-molecular-weight fragments which have high vapor pressure at room temperature.

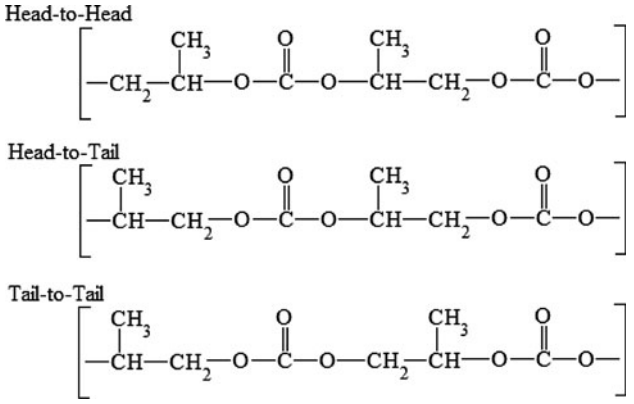

Fig. 1. The local structure of poly(propylene carbonate) can exist as HH, TT or HT. HH and TT are essentially the same structure with a different choice of reference plane. HT is the most desirable, as its alternating structure allows self-propagating decomposition to occur by chain unzipping.

PPC is an attractive sacrificial material for microelectronics because it decomposes cleanly into low-molecular-weight products with little residue in inert and oxygen-rich atmospheres. PPC has been patterned by reactive-ion etching and photopatterning with ultraviolet (UV) radiation when a photo-acid generator (PAG) was mixed with the PPC.[1,5–7] The acid catalyzes decomposition of the PPC at temperatures below that of pure PPC.[1,5–7] The patterned PPC structures can be overcoated with Avatrel, polyimide, SU8, spin-on glass or plasma-enhanced chemical vapor (PECVD)-deposited SiO_2. Air cavities are formed by decomposing the PPC patterns and letting the products diffuse through the overcoat, thus leaving a gaseous void. Because PPC has a low decomposition temperature (180°C), air cavities can be built on tetrabromobisphenol A (FR4), bismaleimide triazine (BT), other thermoset epoxy-fiberglass substrates, and printed circuit boards (PCBs).

Acid-catalyzed decomposition of PPC enables low-temperature, selective patterning, leaving unexposed PPC regions on the substrate while decomposition occurs in the exposed regions. The decomposition

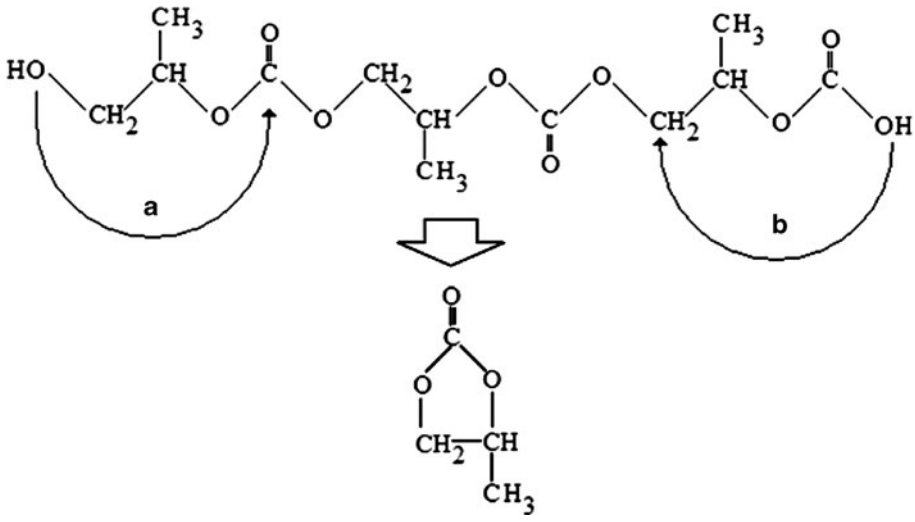

Fig. 2. Chain unzipping of an acid-activated termination can proceed via (a) alkoxide biting or (b) carbonate biting. Both mechanisms yield cyclic propylene carbonate as the primary product with fragment products of carbon dioxide, acetone, and other low-molecular-weight species.

results in evaporation of the reaction products at temperatures as low as 60°C.[8,22] Therefore, photosensitive PPC requires fewer processing steps for patterning and etching than nonphotosensitive PPC. The decomposition characteristics of PPC depend on the interactions among PPC, the casting solvent, and the presence of other contaminants.

Efforts to improve the thermal stability of PPC involve increasing the molecular weight,[23] changing the backbone structure,[10,14,18,19] adding cross-linking,[24,25] and use of additives that prevent decomposition. Enhancement of the thermal stability of PPC has been reported by end-capping the polymer chains[21,26–28] to inhibit initiation of the decomposition mechanism or hydrogen bonding to carbonyl oxygens to suppress propagation of the degradation reaction.[29–35] The most successful attempts to improve the thermal stability have inhibited both initiation and propagation of the decomposition. Phosphorus oxychloride, acetic anhydride, ethylsilicate, benzoyl chloride, and maleic anhydride are known to increase the PPC thermal stability by end-capping terminal alcohols and preventing reaction initiation.[21] Alternative efforts focused on suppressing the self-propagating decomposition, termed unzipping, have used structures capable of hydrogen-bonding to the carbonyl oxygen and thus preventing propagation of the decomposition. These include octadecanoic acid,[31] calcium stearate,[30] montmorillonite,[34,36] and organoclays.[32]

Copper dissolution into polymer and dielectric films has been previously reported for other polymeric materials but not for PPC. Low concentrations of copper compounds have been reported to decrease the polymer stability in nearly all blends of polymers, and accelerate both oxidative and nonoxidative decomposition.[37] The cuprous/cupric oxide mixture acts as an effective oxidation/reduction couple. Low concentrations of copper trifluoromethanesulfonate suppress decomposition of cyclic propylene carbonate under bias,[38] but PPC has not been studied. Copper uptake into MeCl[39] and copper dissolution in GBL have also been reported.[40] The interaction of copper with PAGs, including diaryliodonium salts such as 4-methylphenyl[4-(methylethyl)phenyl] iodoniumtetrakis (pentafluorophenyl)borate (FABA), occurs by Cu(II) reduction to Cu(I) and oxidization of an alcohol to a ketone.[41] Cu(I) interacts with diaryliodonium salts to form a short-lived organocopper intermediate with both radical and ionic properties. In the presence of nucleophilic species, cationic polymerization may occur. Copper is unique in interacting with diphenyliodonium salts, as no effect was seen with salts of Ni(II), Cr(III), Fe(II), Ag(I), Co(II), Mn(III) or Pd(II).[41]

In this paper, the decomposition characteristics of solvent-cast, photosensitive PPC films containing trace levels of copper ions are reported. Copper ions are shown to interfere with the thermal and acid-activated decomposition of PPC, resulting in higher decomposition temperatures. Self-aligned PPC patterns encapsulating copper traces are described without use of a photolithographic patterning or alignment step. The quantity of copper needed to alter the PPC decomposition temperature has been evaluated, along with its effect on patterning characteristics. Copper appears to stabilize the carboxylic acid termination on the PPC backbone and inhibit decomposition through the unzipping mechanism.

EXPERIMENTAL PROCEDURES

Polymer solutions were prepared by mixing PPC, PAG, and solvent. High-molecular-weight poly(propylene carbonate) (M_W = 218,000 g/mol) was obtained from Novomer (Waltham, MA). Rhodorsil-FABA PAG, and FABA was obtained from Rhodia (Boulogne-Billancourt, France), while TCE, MeCl, and GBL were obtained from Sigma-Aldrich (St. Louis, MO). PPC (20 wt.%) was dissolved in solvent with 0.600 wt.% PAG (3.00 wt.% relative to solid polymer) and kept on a bottle roller for 24 h to ensure a good mixture.

A Ti layer with a thickness of 200 Å and a Cu layer with a thickness of 2500 Å were deposited on silicon wafers sequentially using a CVC DC sputterer with Ti serving as an adhesion layer. Prior to spin-coating the Cu substrate samples with PPC solution, the wafer was rinsed in a solution of dilute sulfuric acid (10% H_2SO_4 by volume). Silicon wafers were also rinsed to ensure fair comparison between substrates. No additional treatment, such as removal of the surface oxide with hydrofluoric acid (HF) solution, was performed on the Si substrates. Surface oxide was cleaned from one of the silicon substrates to test bare silicon, but no difference between bare and natively oxidized surfaces was observed.

Copper patterns for evaluation of diffusion effects and copper uptake measurements were patterned by sputtering a seed layer and electroplating lines to a desired thickness. Pattern extension lengths were measured by profilometry and optical microscopy. Copper removal was estimated by profiling the copper line surface before coating with PPC and after stripping PPC. The difference in surface profiles was calculated as the copper thickness removed. PPC films were dried for 2 h in ambient air before stripping with acetone.

Films for analysis in thermogravimetric analysis (TGA) experiments were dispensed on wafers using a CEE spin-coater and then soft-baked on a hotplate at 70°C for 20 min. Following the soft-bake, sections of polymer film were removed from the wafer surface using a razor blade and tweezers and loaded into the TGA tin. Dynamic TGA scans were performed using a Q50 thermogravimetric analyzer from TA Instruments (New Castle, DE). PPC films were decomposed on a platinum tin in a chamber purged with nitrogen with flow rates of 40 mL/min on the balance and 60 mL/min on the sample at a temperature ramp rate of 0.5°C/min. The microbalance was re-zeroed prior to each experiment.

PPC films containing copper were analyzed by inductively coupled plasma (ICP)-optical emission spectroscopy (OES) by first spin-coating polymer solution on a copper-coated wafer, soft-baking for 10 min at 110°C, redissolving PPC in GBL, and pipetting from the surface. This process was repeated for PPC with 2.00 wt.% Rhodorsil-FABA on copper and silicon and for PPC with 2.0 wt.% H_2SO_4 on copper. To compare copper uptake by solvent alone, GBL was heated at 110°C on a copper-coated wafer for 10 min and pipetted off the wafer surface for analysis. Solutions from the dissolved films were analyzed using a Teledyne Leeman Prodigy ICP-OES system, where samples were diluted 10:1 in dimethylacetamide for analysis. Calibration was performed prior to analysis with 1 ppb, 3 ppb, 5 ppb, 20 ppb, 50 ppb, and 100 ppb standards.

Films were analyzed by Fourier-transform infrared (FTIR) spectrometry using a Nicolet Magna 560 Spectrometer. Prior to collecting each spectra, a background spectra was taken through a clean KBr disk in a nitrogen-filled chamber purged at 50 mL/min for 1 h after sample loading. After background collection, a polymer film was coated onto KBr via pipette, dried for 20 min on a hotplate at 110°C, and loaded into the chamber, and the chamber was purged for 1 h with nitrogen. Spectra were collected at a spacing of 2 cm^{-1} and averaged over 512 scans. PPC dissolved in GBL with 2.00 wt.% Rhodorsil-FABA PAG was dispensed directly onto the KBr disk. Copper-doped films were cast from PPC redissolved in GBL from a copper wafer surface as described for ICP-OES analysis. After 72 h, the "copper-rich" portion of the solution segregated into a blue phase, which was pipetted and dispensed onto a KBr film in the same manner as other FTIR samples.

The copper-rich portion precipitated into a solid after 6 months in solution. Elemental analysis of this precipitate was performed by energy-dispersive x-ray (EDX) spectrometry using a Hitachi VP SEM S-3700N. Samples were sputtered with a 50-Å layer of gold prior to analysis to improve surface charging. Boron, copper, and gold were calibrated using elemental standards, while oxygen was calibrated with an SiO_2 standard, carbon was calibrated with a $CaCO_3$ standard, and sulfur was calibrated with an FeS_2 standard.

RESULTS

It was observed that, when a PPC and PAG solution in GBL was coated onto a copper surface, dried, and heated, the PPC in contact with the copper surface decomposed at a substantially higher temperature than the PPC not exposed to copper. The change in decomposition temperature for the copper-contacted region was ca. 50°C. A similar shift in decomposition temperature was observed for PPC and PAG mixtures in GBL which were exposed to ultraviolet (UV) radiation. In the first portion of the "Results" section, the PPC decomposition characteristics are described, followed by the self-patterning aspect of this phenomenon.

PPC Decomposition in the Presence of Copper

Exposing a PPC and PAG formulated film to a copper surface promotes uptake of copper into the film, resulting in a decrease in the copper metal thickness and a change in color of the PPC film. The PAG and GBL solvent provided a corrosive environment for the copper, resulting in oxidation of copper, likely caused by reduction of dissolved oxygen. The amount of copper taken up into the PPC film was estimated based on the change in copper thickness after removal of the PPC from the surface, as measured by profilometry. The material properties and summary calculations are presented in Table I. Calculations are shown for mass, moles, molecules, and carbonyl group per film area. PPC density (1.3 g/cm[342–45]) and copper density (8.96 g/cm^3) were based on bulk properties. The results show that 6 ng copper was oxidized from the surface per mm^2 of surface area. The oxidation and dissolution of copper creates a very dilute copper concentration within the PPC film. If the copper were homogeneously distributed within the PPC film, the mass fraction of copper relative to PPC would be 0.006. Calculations of carbonyl concentrations were based on the molecular weight of one monomer of propylene carbonate (M_W = 104 g/mol) in the PPC

Table I. Material properties and calculations for estimating copper uptake concentration

	Symbol	PPC	Copper	Units
Layer thickness	t	10	0.0067	μm
Density	ρ	0.0013	0.0090	ng/μm^3
Mass per area	$t{\cdot}\rho$	0.013	0.00006	ng/μm^2
Molecular weight	M_W	2.2×10^{14}	6.4×10^{10}	ng/mol
Moles per area	$t{\cdot}\rho/M_W$	6.0×10^{-17}	9.4×10^{-16}	mol/μm^2
Molecules per area	$N_A{\cdot}t{\cdot}\rho/M_W$	3.6×10^{7}	5.7×10^{8}	molecule/μm^2
Monomers per area	$N_A{\cdot}t{\cdot}\rho/M_W$[a]	7.5×10^{10}	–	C=O/μm^2

[a]Monomer/carbonyl concentration based on molecular weight of one monomer of propylene carbonate (M_W = 104 g/mol) in the PPC backbone.

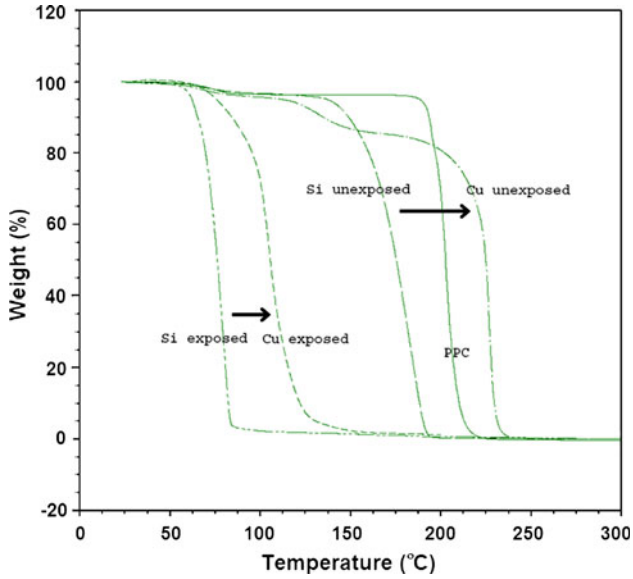

Fig. 3. Dynamic TGA plots for PPC films in GBL cast on a copper surface (exposed to copper) and cast on silicon (not exposed to copper) with and without UV exposure compared with decomposition of neat PPC without UV exposure.

backbone (~2100 monomers for 218,000 g/mol). The atomic concentration ratio was ~1 copper ion per 100 carbonyl or monomer units. This small number of copper ions per polymer strand is consistent with the hypothesis that the copper may be acting to stabilize the polymer ends so as to inhibit the decomposition, as shown in Fig. 2.

The stabilization of PPC (GBL solvent) against thermal decomposition in the presence of copper was examined by TGA. Dynamic TGAs (0.5°C/min) were carried out on UV-exposed and unexposed PPC (with PAG included in the casting mixture) exposed to copper and not exposed to copper (i.e., cast on silicon), as shown in Fig. 3. All exposed films received a UV dose of 1 J/cm^2 (λ = 248 nm) while on the silicon or copper substrates. A majority of the decomposition for the films cast on silicon occurred between 60°C and 90°C. However, PPC cast from GBL on copper decomposed at a much higher temperature, analogous to the unexposed samples described above, between 60°C and 120°C.

UV exposure of the PPC with PAG results in a lower decomposition temperature because the photogenerated acid catalyzes decomposition of the PPC at less than 70°C, as shown in Fig. 3. The PPC mixture in contact with silicon and exposed to UV radiation is labeled "Si exposed," and the sample in contact with copper is labeled "Cu exposed." The photogenerated acid attacks the carbonyl (weak base), resulting in destabilization of the PPC at a relatively low temperature. Figure 3 also shows the thermal decomposition of neat PPC (labeled "PPC"). PPC with PAG (not exposed to copper) decomposes at a lower temperature than neat PPC because the thermal activation of the PAG generates an acid which catalyzes PPC decomposition. The PPC samples in contact with silicon and copper are labeled "Si unexposed" (to UV radiation) and "Cu unexposed." Thus, the decomposition temperature of the PAG-loaded sample (no UV exposure) was set by the thermal decomposition temperature of the PAG creating the acid. PPC cast from GBL on copper showed a much higher decomposition temperature (complete decomposition at ca. 230°C) than the samples not exposed to copper. The copper-exposed PPC also showed a higher decomposition temperature than neat PPC due to the stabilizing effect of dissolved copper ions, as discussed later. The decomposition temperature of PPC with PAG exposed to copper was higher than that of PPC from the silicon substrate by 30°C for UV-exposed samples and by more than 50°C for unexposed samples.

There was a small change, ca. 10%, in PPC weight (Fig. 3) when the PPC was exposed to a copper surface between 120°C and 160°C, prior to the major change in weight at 230°C. This small change in weight occurred at a temperature lower than for neat PPC or PPC on silicon. The nature of this small drop in mass was investigated by analyzing the molecular weight of the decomposition products using electron impact mass spectrometry. Previous studies have shown that the molecular weights of the PPC decomposition fragments were (in order of intensity) 57 *m/z*, 43 *m/z*, 58 *m/z*, 44 *m/z*, and 87 *m/z* (mass to charge). The products of PPC at 43 *m/z*, 44 *m/z*, 57 *m/z*, 58 *m/z*, and 87 *m/z* were assigned to fragmentation of propylene oxide, carbon dioxide, fragmentation of propylene carbonate, acetone, and fragmentation of propylene carbonate, respectively.[7] The mass spectra of the products evolved from the PPC on copper not exposed to UV radiation at 140°C, 160°C, and 180°C were virtually identical to the mass spectrum of neat PPC at its decomposition temperature and to that of PPC on silicon. The spectrum showed the same five dominate peaks at 57, 43, 58, 44, and 87 (in order of intensity). Thus, the small weight loss for PPC in contact to copper decomposed at 140°C is believed to be caused by creation of a small amount of acid from an interaction between the copper and PAG or a change in the end-groups by the copper. While copper suppresses the decomposition of a majority of the PPC (higher decomposition temperature), the creation of a small amount of acid at 140°C would cause some to decompose as if it were exposed to UV radiation. This small amount of PPC on copper decomposition is reflected in the copper imaging results later in this section, where the copper-coated film lost about 10% of its thickness at relatively low temperature (1 μm of a 10-μm-thick film).

The PPC films cast from MeCl and TCE on copper did not show a significant shift in the TGA curves compared with the non-copper-exposed films. However, thermal patterning was still observed, although to a lesser extent than with GBL. There appears to be a suppression of the thermal decomposition of the

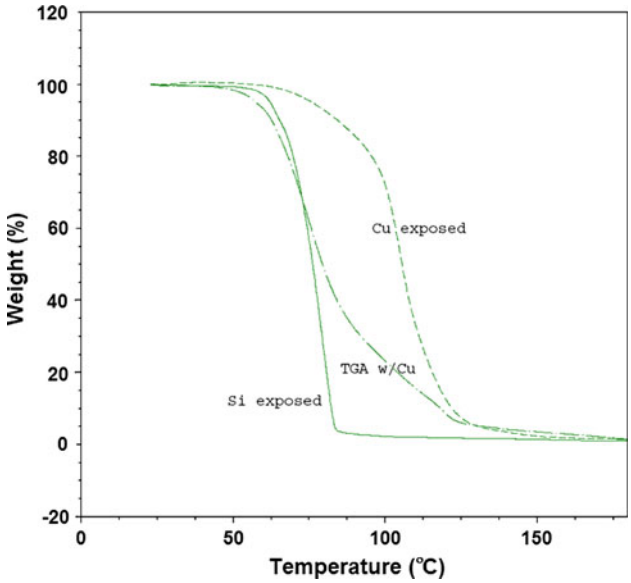

Fig. 4. Dynamic TGA plots for exposed PPC films on copper and silicon substrates cast from solutions dissolved in GBL. Samples were exposed to 1 J/cm^2 UV at λ = 248 nm and decomposed in nitrogen at a heating rate of 0.5°C/min. The curve labeled "with Cu" was cast from TCE (no GBL) and had copper mixed with the polymer material during the TGA experiment.

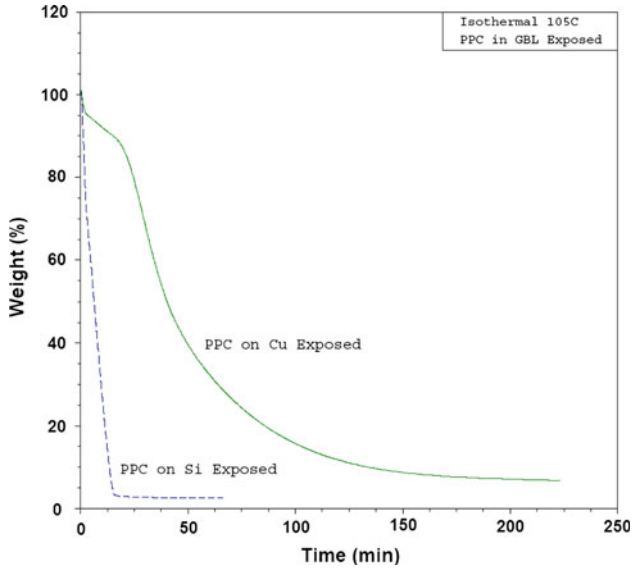

Fig. 5. Isothermal TGA curve at 105°C showing mass fraction versus time for PPC films cast from GBL-dissolved PPC with 3 wt.% PAG on silicon and copper.

PPC in the MeCl and TCE, however to a lesser extent than for GBL. The effect was easily seen in patterning experiments (described later in this section), however the effect was more difficult to show by TGA because of the slow TGA scan rate. The effect is demonstrated in Fig. 4. A PPC sample was mixed with copper particles, exposed to UV radiation, and examined by TGA (Fig. 4 "TGA w/Cu"). This was done by scraping the film and copper from the wafer surface to provide a continuous source of copper during the heating cycle. The other two curves are for PPC cast from GBL and exposed to UV radiation, as described above. Initially, decomposition of the TCE cast sample with copper particles proceeded similarly to other films, but then the decomposition slowed dramatically, presumably due to further copper ion uptake into the PPC. Thus, the suppression of PPC decomposition in the presence of copper in TCE (and MeCl) appears to be more sensitive to the amount of copper present, or the uptake of copper occurred to a lesser extent in those solvents.

The suppression of the decomposition temperature due to copper uptake using TCE or MeCl rather than GBL shows that the solvent is a necessary component, but not the determining factor, in the suppression process. The similarities of the decomposition temperature in the TGA results suggest that the solvent assists in uptake of copper ions into the PPC but is not the temperature-changing component. There are several possible reasons for some solvents to be more effective at shifting the decomposition temperature. The incorporation of copper ions into the PPC requires oxidation and dissolution of the copper. The rate and amount of copper taken up into the PPC can be affected by the amount of residual solvent, concentration of adsorbed oxygen (contributing to copper oxidation), and ability of the solvent to stabilize copper ions in the PPC. These factors are currently under investigation.

To further study the self-patterning process of PPC for air-clad transmission-line applications, isothermal TGAs were performed, as shown in Fig. 5 for GBL-cast PPC films on silicon and on copper after UV exposure. The samples were heated at a ramp rate of 100°C/min to 105°C/min and held at that temperature while the mass was monitored. The film cast on silicon showed an immediate weight loss, followed by a period of time when decomposition occurred at a constant rate. Complete decomposition occurred in 15 min. The film cast on copper initially lost a small weight fraction, about 10%, at a lower temperature, most likely due to the early decomposition contributed by the presence of copper. Decomposition began about 20 min after achieving the dwell temperature. The observation shows a different PPC decomposition rate between these two samples at the analysis temperature.

A series of isothermal TGAs were obtained to better understand the PPC suppression. Dynamic TGAs can distort certain thermal effects, because temporal and thermal effects are combined in a single scan, whereas isothermal TGAs involve only temporal effects at a specific temperature. Isothermal TGA data for PPC with PAG samples exposed to copper and not exposed to copper at 140°C, 160°C, and 200°C are shown in Figs. 6–8, respectively. Figure 6 shows that the weight percentage of PPC removed from the Cu substrates dropped quickly to 96.8% in the first 3 min, while the PPC removed

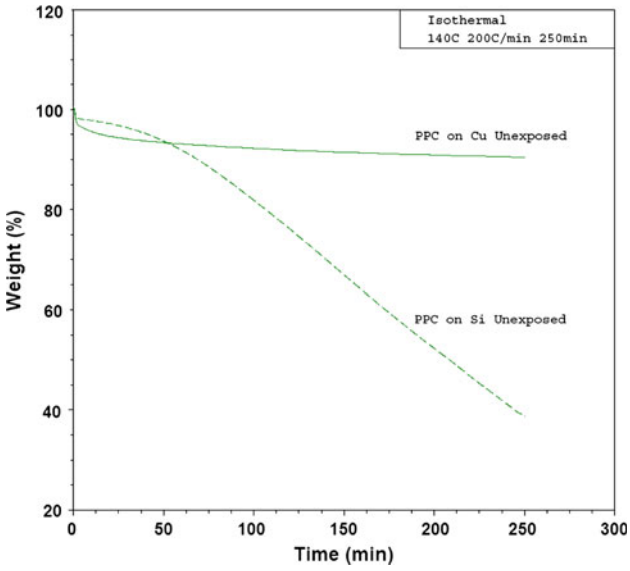

Fig. 6. Isothermal TGA curve at 140°C for a PPC film removed from either silicon or copper substrates without UV exposure.

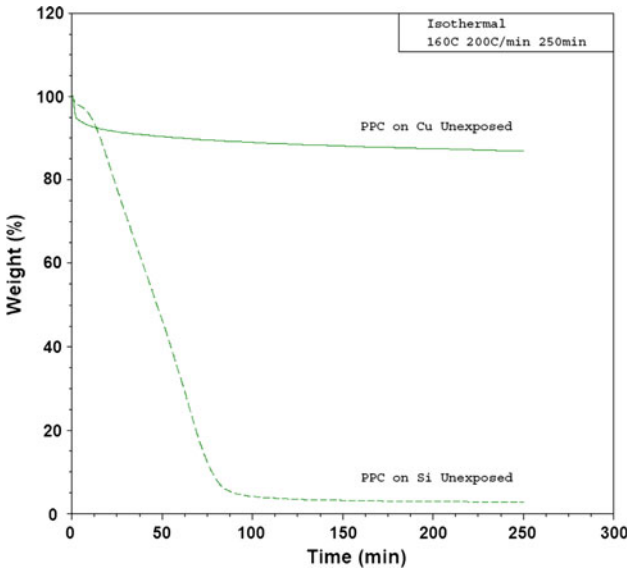

Fig. 7. Isothermal TGA curve at 160°C for a PPC film removed from either silicon or copper substrates without UV exposure.

from the Si substrates decomposed at a nearly consistent rate. The decomposition of the PPC exposed to copper slowed after 9 min, with less than 10% weight loss after 250 min at 140°C, in agreement with the results of dynamic TGA described above, where the copper stimulates a small amount of PPC decomposition at a relatively low temperature. When performing isothermal TGA at 160°C (Fig. 7), the PPC exposed to copper had a weight loss of 5.7% after 4 min, and a total of 13.1% after 250 min at 160°C. In contrast, the PPC with PAG not exposed to copper decomposed completely at the end of the measurement time. At 200°C, as shown in Fig. 8,

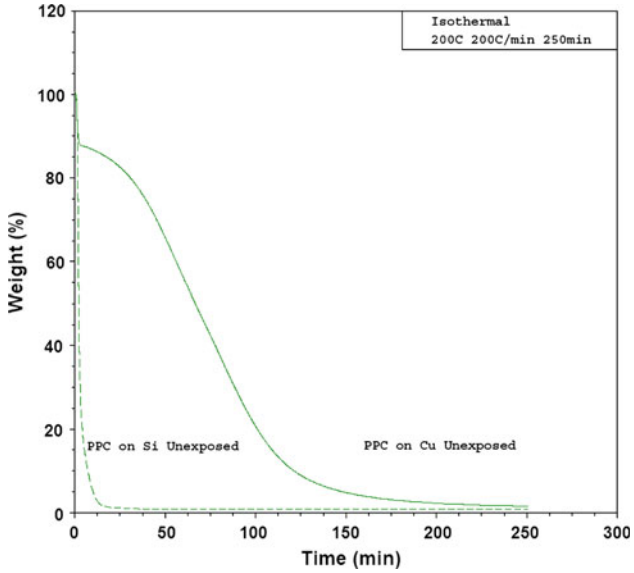

Fig. 8. Isothermal TGA curve at 200°C for a PPC film removed from either silicon or copper substrates without UV exposure.

the PPC not exposed to copper rapidly decomposed and fully decomposed after 14 min with less than 1.5% weight remaining.

FTIR spectra for the PPC films dissolved in GBL are shown in Fig. 9. No significant difference is observed between the film containing 2.00 wt.% FABA and the film without PAG. The spectrum for copper-containing PPC shows a slight decrease in the height of the peaks attributable to the terminal carboxylic acid groups (at 3000 cm^{-1} and 1120 cm^{-1}). The peak at 1120 cm^{-1} is indicative of a secondary alcohol and may be due to the interaction of the terminal carboxylic acid groups with copper. However, it is difficult to say with confidence if these peaks capture the copper interaction, as the relatively weak peak near 3000 cm^{-1} may be obscured by C–H bonds, and the peak at 1120 cm^{-1} may arise from residual GBL in the polymer matrix. FTIR spectra for the PPC films cast in methylene chloride or TCE do not show this difference.[9]

Self-Aligned, Lithographic Patterning of PPC on Copper Using the Increased Thermal Stability of the PPC-PAG-Cu Mixture

PPC patterns on copper lines were created by exposing the PPC with PAG films cast from GBL to UV irradiation (1 J/cm^2). The copper was oxidized and dissolved into the PPC during solvent soft-bake and postexposure bake, forming a copper-ion-rich PPC layer which inhibits acid-catalyzed decomposition of the PPC. This process is summarized in Fig. 10, which shows the maskless patterning of PPC on copper lines. The cross-section build-up process starts with a copper line on a silicon wafer or epoxy-fiberglass substrate. The copper line is then coated with PPC and PAG dissolved in solvent.

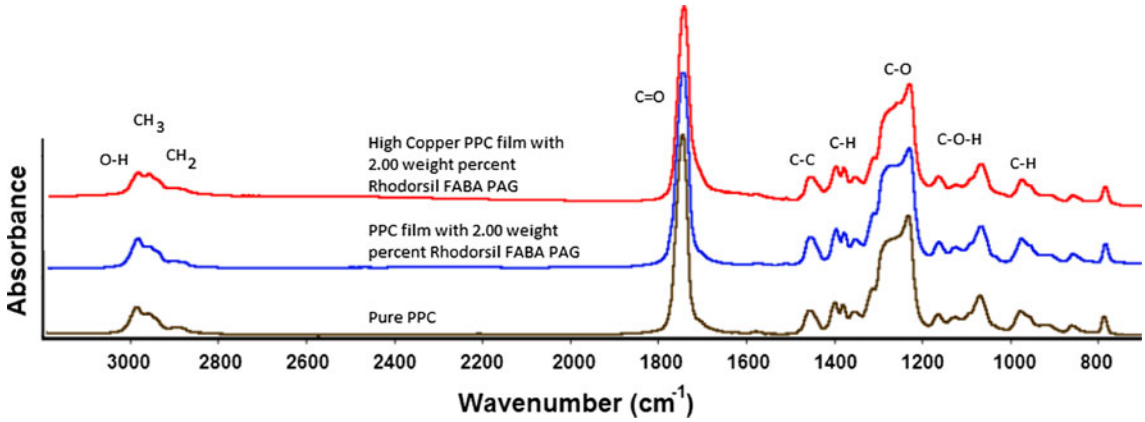

Fig. 9. FTIR spectra for PPC films dissolved in GBL containing 2.00 wt.% FABA PAG. Peaks ca. 1750 cm^{-1} (C=O) and ca. 1250 cm^{-1} (C–O) are attributable to carbonate units. Peaks ca. 2980 cm^{-1} (CH_3), 2900 cm^{-1} (CH_2), 1450 cm^{-1} (C–C), 1350 cm^{-1}, and 980 cm^{-1} (CH) are attributable to propylene units. Peaks ca. 2980 cm^{-1} (O–H) and ca. 1120 cm^{-1} (C–O–H) are attributable to terminal carboxylic acid and show decreased intensity in copper-rich PPC.

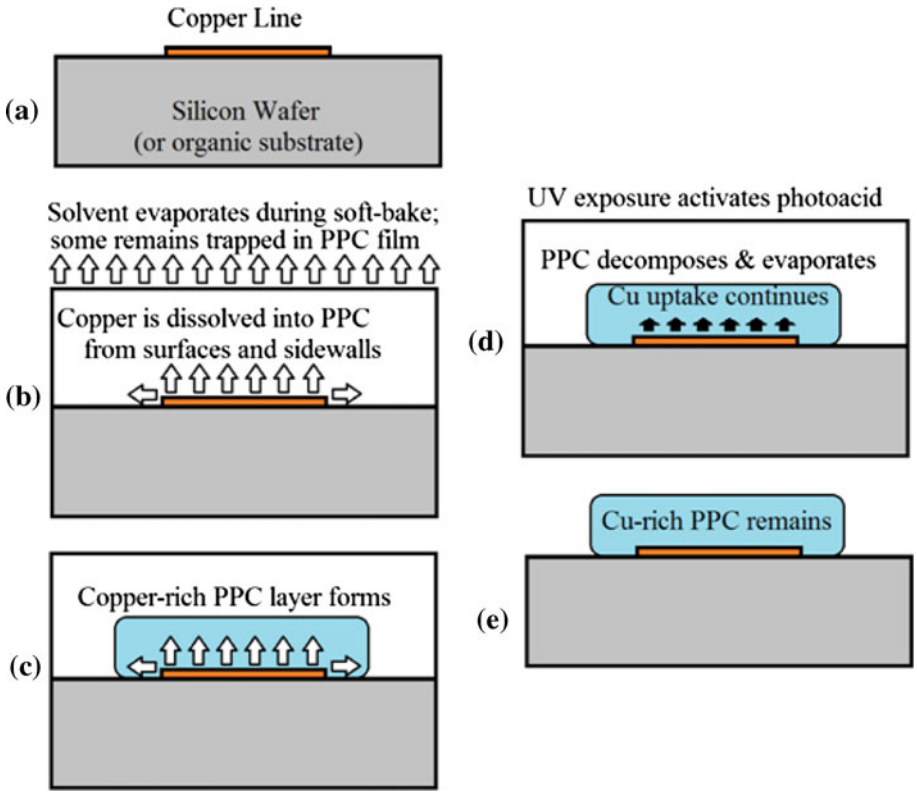

Fig. 10. Process summary of maskless patterning of PPC on copper lines. The cross-section build-up process shows (a) a copper line on a substrate which is coated with PPC dissolved in solvent which is heated on a hotplate to ca. 100°C, (b) evaporating solvent and dissolving copper from the line surface and edges into PPC, where (c) copper diffuses into PPC to form a copper-rich layer, which (d) continues to take up copper and does not decompose when the film is UV exposed, (e) leaving a copper-rich PPC layer encapsulating the line.

The solvent was evaporated by soft-baking the sample at 100°C. During spin-coating and heating, copper was oxidized and dissolved from the copper surface and taken up into the solvent/PPC/PAG film. The copper-rich PPC layer remains because, at the exposure temperature, it decomposes much more slowly than the copper-free regions of PPC. The pattern can then be encapsulated with an overcoat dielectric support material and ground conductors to build electrical lines. The self-patterning capability of photosensitive PPC is valuable because it eliminates masking and alignment steps and simplifies processing, potentially improving cost and yield.

Table II. PPC film thickness before and after patterning and lateral spreading of PPC line edge from copper edge after patterning

Solvent	Initial PPC Film Thickness (μm)	PPC Thickness After Patterning (μm)	Lateral Spreading from Copper Edge (μm)	Development Time (min)	Development Temperature (°C)
MeCl	10.8	7.4	9.8	70	78
TCE	10.0	5.6	4.8	41	80
MeCl	−10.8	6.7	3.9	3.0	98
TCE	10.0	5.4	–[a]	3.0	100
GBL	9.8	−8.1	3.0	3.0	115
GBL[b]	−10.2	9.1	31.7[c]	3.1	115

Increased pattern development temperature reduces line edge spreading. [a]Retraction of PPC from copper line edge of up to 23 μm; see Figs. 11–15. [b]Copper line was electroplated 17 μm thick. [c]Increased lateral spreading is due to higher copper uptake from thicker copper line.

The PPC film thickness before and after dry-developing and lateral extension of PPC features was measured by surface profilometry and optical microscopy, as reported in Table II. All films were initially 10 μm thick. The films were completely decomposed on silicon, and partially decomposed on copper. The films cast from TCE were developed at 80°C for 41 min and 100°C for 3 min, while the films cast from MeCl were developed at 78°C for 70 min and 98°C for 3 min. Both films cast from GBL were dry-developed at 115°C for 3 min. The copper film thickness was ca. 250 nm for all films, except one PPC film cast from GBL on a 17-μm-thick electroplated copper line. Figure 11 shows a plan-view optical microscope image of PPC lateral extension when cast from GBL on a 17-μm-thick copper line. PPC remained intact on the silicon surface with lateral extension of 31.7 μm from the copper line edges. Regions labeled "silicon wafer surface," "PPC lateral extension," and "copper coated with PPC" in Fig. 11 are the same in subsequent images. Figure 12 shows a plan-view optical microscope image of PPC cast from MeCl at the edge of 250-nm copper after 70 min of development at 78°C. The lateral extension was 9.8 μm. Figure 13 shows a film cast from MeCl after 3 min of dry-development at 98°C, where the lateral extension decreased to 3.9 μm while the partially decomposed region extended almost 10 μm from the copper line edge. A plan-view optical microscope image of PPC cast from TCE and developed for 41 min at 80°C is shown in Fig. 14. The lateral extension was 4.8 μm. Figure 15 shows a plan-view image of PPC cast from TCE and developed at 100°C for 3 min. No lateral extension was observed but rather retraction of PPC up to 21.2 μm from the copper line edge.

The thickness of the copper removed from the copper line surface due to PPC uptake was measured using surface profilometry. The surface profile scans of a copper line before PPC coating and after PPC coating then stripping are shown in

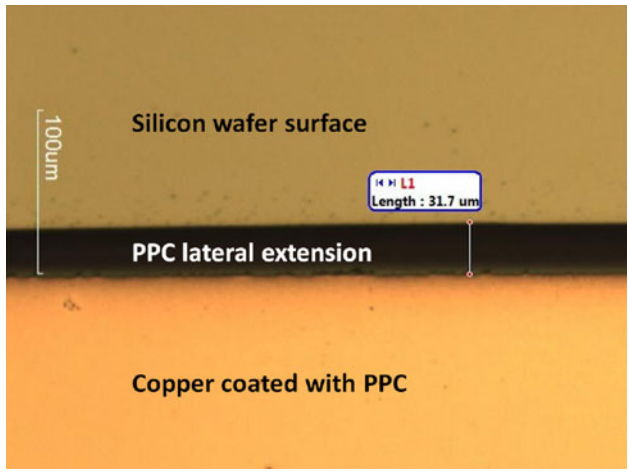

Fig. 11. Plan-view optical microscope image of 31.7 μm PPC lateral extension from copper line edge for PPC film cast from GBL after 3.1 min postexposure bake at 115°C. The copper line is 17 μm thick on silicon and allows copper uptake from the sidewall into PPC.

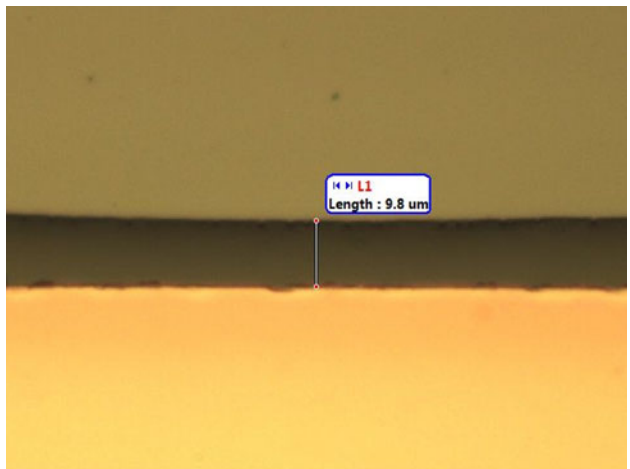

Fig. 12. Plan-view optical microscope image of 9.8 μm PPC lateral extension from copper line edge for PPC film cast from MeCl after 70 min postexposure bake at 78°C.

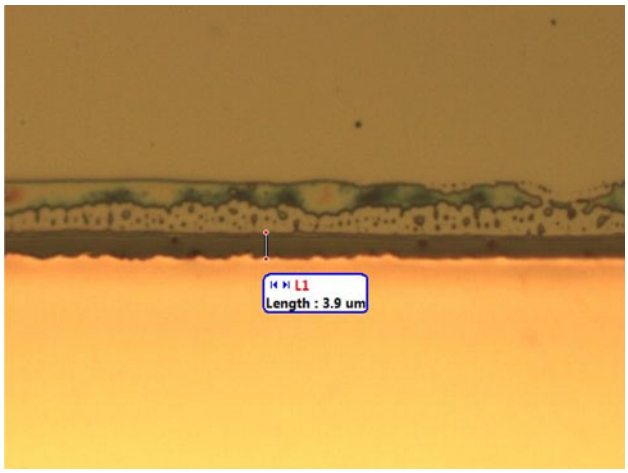

Fig. 13. Plan-view optical microscope image of 4.8 μm PPC lateral extension from copper line edge for PPC film cast from TCE after 41 min postexposure bake at 80°C.

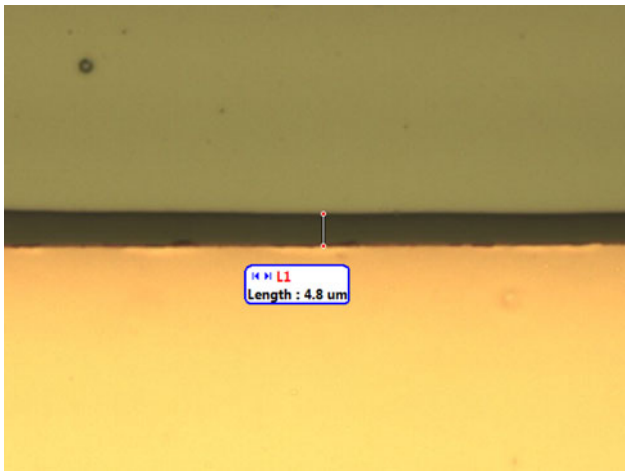

Fig. 14. Plan-view optical microscope image of 3.9 μm PPC lateral extension from copper line edge for PPC film cast from MeCl after 3.0 min postexposure bake at 98°C. Residue due to incomplete decomposition extends 10 μm from copper line edge.

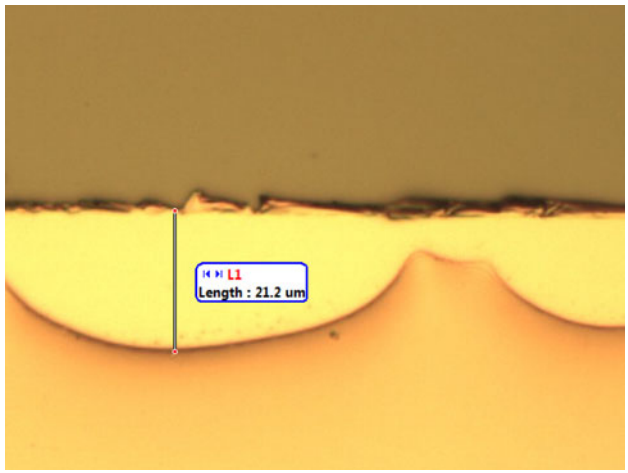

Fig. 15. Plan-view optical microscope image of 21.2 μm PPC retraction from copper line edge for PPC film cast from TCE after 3.0 min postexposure bake at 100°C.

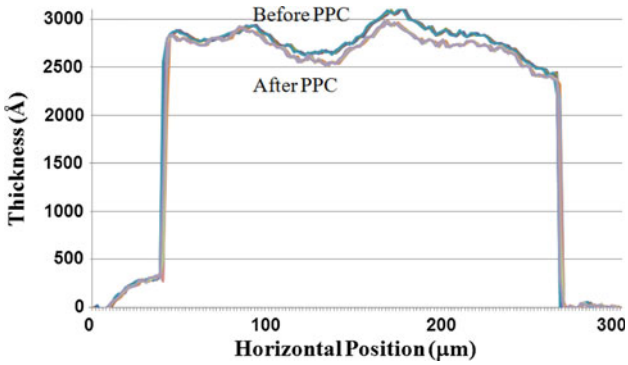

Fig. 16. Copper removed from line surface by copper. Shown are surface profiles of a copper line before coating with PPC and after stripping PPC. The average thickness removed from the copper line surface between 150 μm and 850 μm was 67 Å and is used for calculations shown in Table I.

Fig. 16. The average copper thickness decreased by 67 Å across the top of the line surface. Copper removed from sidewalls was not measured. The decreased thickness is primarily due to oxidation and dissolution of copper ions into PPC. However, part of the decrease may have occurred when the PPC was dissolved in acetone.

Metal uptake into the PPC film was analyzed using ICP-OES to analyze the PPC solution, while energy-dispersive x-ray spectroscopy (EDS) was used to analyze elemental content of the salt that precipitated out of the solution. Shown in Table III are the results from ICP-OES performed on GBL, PPC dissolved in GBL, PPC dissolved in GBL with PAG on silicon, PPC dissolved in GBL with PAG on copper, and PPC dissolved in GBL with H_2SO_4 on copper. Elevated levels of copper were seen for films cast on copper surfaces, with the highest concentrations observed in the presence of an acid. The atomic and mass percentages of each of these elements characterized by EDS are summarized in Table IV. Among all the elements detected, boron was from the photoinitiator while sulfur was believed to come from the sulfuric acid cleaning done before the application of PPC. Most importantly, a significant amount of copper, 15.04 at.% or 4.18 wt.%, was observed.

Self-patterning of PPC around copper is a valuable processing step when properly integrated into a process flow. Copper lines connected by vias into the substrate may easily be encapsulated with self-patterning PPC, but build-up processes require windows in PPC for electrical connection. This is illustrated in Fig. 17, where self-patterned PPC is shown compared with masked PPC. In the self-patterned region, lateral extension from the copper edges was seen. In the masked PPC region, the dark region of "lateral extension" was actually the

Table III. Metals content by ICP-OES for solutions of (1) GBL, (2) PPC dissolved in GBL, (3) PPC dissolved in GBL with 2.00 wt.% FABA PAG deposited on silicon, (4) PPC dissolved in GBL with 2.00 wt.% Rhodorsil FABA PAG deposited on copper, and (5) PPC dissolved in GBL with 2.0 wt.% sulfuric acid deposited on copper

Element	γ-Butyrolactone (GBL) on Copper	PPC-GBL on Copper	PPC-GBL-FABA on Silicon	PPC-GBL-FABA on Copper	PPC-GBL-H_2SO_4 on Copper
Cu	540	1000	20	50,000	5000
B	200	660	3000	5000	1400
Ni	<10	<10	<10	40	1100
Na	<10	80	<10	200	1000
Co	<10	20	30	90	30
Cr	14	12	<10	14	70
Fe	<10	<10	<10	16	70
Al	<10	<10	<10	90	60
Zn	<10	<10	18	400	20
Mo	18	18	16	30	50
Mg	<10	<10	<10	12	40
Mn	14	14	14	16	14
Ca	<10	<10	<10	50	<10
Ba	<10	<10	<10	<10	<10
Cd	<10	<10	<10	<10	<10
K	<10	<10	<10	<10	<10
Pb	<10	<10	<10	<10	<10
Sn	<10	<10	<10	<10	<10
Li	<10	<10	<10	<10	<10
Pd	<10	<10	<10	<10	<10

Table IV. EDS analysis results for elements and relative percentages

Element	Atomic Percent	Weight Percent
B	14.8	24.2
C	4.5	6.6
O	53.2	58.8
S	11.1	6.1
Cu	15.0	4.2
Au	1.4	0.1

rounding of the pattern edge due to low contrast. The rounding of features was present in both regions, but the self-patterned region was broader due to the uptake of copper.

Shown in Fig. 18 is an identical structure to Fig. 17 except the probe pads on the left side of the image are protected by a 200-Å-thick layer of titanium to prevent copper interaction with PPC. Complete decomposition of PPC from the probe pad surface was observed. At the boundary of the titanium layer and the photomask pattern, PPC extended on copper slightly, apparently due to misalignment, although this might be due to lateral diffusion of copper.

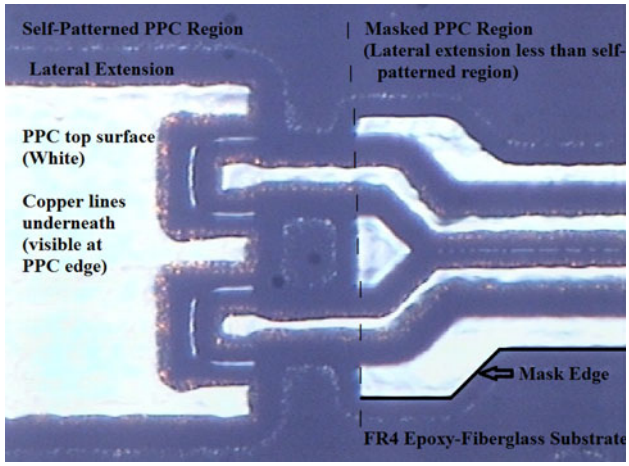

Fig. 17. Optical microscope image of self-patterned PPC and masked PPC on copper probe pads on an FR4 epoxy-fiberglass substrate. PPC is clear but appears white in this image due to reflectance of light and clear at the edges. PPC on the left self-patterns around the copper surface. PPC on the right was patterned through a mask and shows slight lateral extension (due to feature softening above the glass-transition temperature). Lateral extension is more pronounced from the line edge in the self-patterned region because copper from the sidewall diffuses into and stabilizes PPC.

DISCUSSION

Copper uptake from the copper surface into the solvent-cast PPC films was evident from surface profiles, metals analysis, and the color change in the PPC film. The mechanism of copper uptake is assumed to be from air oxidation of copper in the acid-laden PPC film followed by dissolution. When PPC was thermally decomposed using the higher decomposition temperature of the copper-loaded region as the means of self-patterning, a PPC film on the copper remained with some extension of the PPC to regions outside the copper pattern.

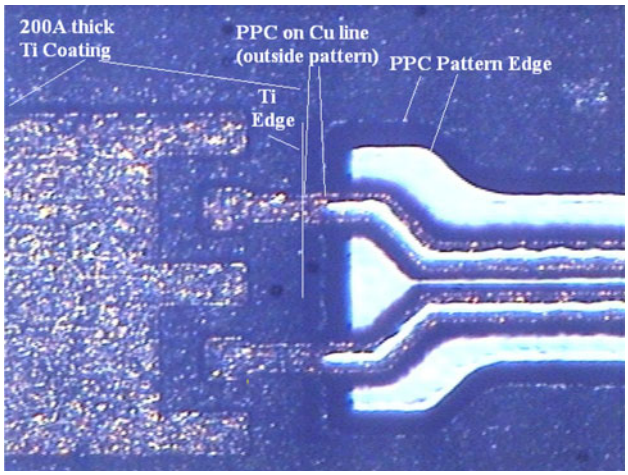

Fig. 18. Optical microscope image of copper probe pads coated with titanium to prevent PPC self-patterning. The titanium barrier layer prevents uptake of copper into PPC, disabling the self-patterning characteristics. As in Fig. 17, the white region is PPC and is masked to form the dog-bone shape encapsulating the copper lines. The copper on the left side of the image has been coated with 200 Å of Ti prior to PPC spin-coating and patterning.

The extent of the lateral extension of the PPC from the edge of the copper line depended on the solvent selection, soft-bake temperatures and development time, and copper layer thickness, as presented in Table II.

Longer interaction time between the copper metal and the PPC film allows for a longer diffusion and reaction time, while higher temperature helps accelerate the reaction. The influence of temperature is most clearly viewed by comparing Figs. 12 and 14. Lateral extension of the film is uniform about 10 μm from the copper line edge for MeCl-cast PPC (Fig. 12) when the development temperature was 78°C. Increasing the development temperature to 98°C decreases the lateral extension to less than 4 μm, but a partially decomposed region about 10 μm from the edge is clearly visible. This may be the portion of the PPC film that initially had low concentrations of copper but in insufficient amounts to suppress decomposition. Slower reaction rates at lower temperature enable copper to diffuse from the higher-concentration region to stabilize the boundary region before the film decomposes. Lateral extension for 4.8-μm TCE-cast films at 80°C becomes recessed from the copper edge by up to 21.2 μm at 100°C, indicating that the copper concentration at the edge of the film was inadequate to suppress decomposition. This illustrates the lower uptake rate of copper into PPC films cast from TCE. Lower development temperature and longer interaction time both increase copper uptake, as evidenced from these images as well as the TGA data in Fig. 4.

Interaction time and diffusion effects are evident not only from lateral extension but also film thickness after patterning on copper, as presented in Table II. GBL films retained the largest fraction of initial film thickness (greater than 80%), followed by films cast from MeCl and TCE. The reason for this difference is unclear. Decreasing the development temperature with a longer development time increased the remaining film thickness, suggesting that longer development time allows copper to migrate from the metal surface further into the PPC film.

The diffusion coefficient of copper ions dissolved in PPC has not been studied here due to the complexity of solvent evaporation rates, temperature, and variability of film characteristics. However, the importance of these variables is clear from the results in Table II and Figs. 11–15. PPC films cast using GBL require longer postexposure bake times and higher temperatures, because GBL has a lower vapor pressure than MeCl or TCE. Higher levels of dissolved oxygen may enhance the copper uptake reaction by oxidizing copper for removal from the surface. GBL is also a good electrolyte and may assist copper ion transport in evenly distributing copper in the film and enhancing thermal stability. No effort was made to measure lateral extension for PPC cast from TCE or MeCl on thick copper lines but would be required for more detailed analysis of copper diffusion into PPC.

TGA measurements show that copper-rich films have greater thermal stability than films cast on other substrates. Slight increases in decomposition temperature were observed for MeCl and TCE, but GBL showed the largest effect, with more than 30°C increase in thermal stability when cast on copper rather than silicon. Especially important is the isothermal decomposition plotted in Fig. 6 for PPC films cast from GBL on silicon and copper. PPC films used in this study were approximately 10 μm thick, which means that a 10% change in weight (0.1 in weight fraction) correlates to a 1 μm change in thickness. Thus, nearly the full thickness of a 10-μm PPC film on bare silicon completely decomposes in 15 min, while 9 μm of PPC remains on copper. This thermal selectivity enables maskless photopatterning of PPC features.

ICP-OES results showed elevated copper levels in films cast on copper compared with silicon. Some copper uptake was observed for the GBL solvent alone and PPC with GBL in the absence of PAG, but the concentrations of copper in acid-containing samples were orders of magnitude larger than for PPC films on bare silicon. Comparison of metals content shows the copper concentration is in excess of boron, a component of the PAG.

PPC patterns did not interact with substrates of silicon, silicon dioxide, epoxy-fiberglass boards, Avatrel, gold, silver, zinc, aluminum, chrome, platinum, titanium, and native (thick) copper oxide. PPC films were also cast onto pre-oxidized copper (via etching with hydrogen peroxide) and patterned, however the patterning was not as sharp as that from a pure copper surface. The difference in patterning characteristics suggests that an elemental copper surface is required to achieve oxidation and

dissolution of the copper ions into the PPC film. The ease of oxidation and solubility of copper ions in PPC also makes it unique in this effect, which accounts for the lack of response with the other metals. The importance of copper uptake into the film is clearly illustrated in Table III.

FTIR results suggest the increased thermal stability may be due to coordination with one or more terminal carboxylic acid groups. The decreased intensity of the peak at 3000 cm^{-1} associated with an O–H bond and at 1120 cm^{-1} associated with a secondary alcohol both suggest an alteration of the chemical structure of the terminal carboxylic acid groups. These units may be chelating copper to immobilize the end-groups, or may even coordinate end-groups to crosslink chains, although no attempts have been made to measure changes in molecular weight. Alternatively, copper may be interacting with carbonyl oxygens but no change in peak intensity at 1750 cm^{-1} is observed because the concentration of copper relative to carbonyl oxygens (1:100) is so low.

The relative quantities of copper and boron as measured by EDS are approximately equal, suggesting that boron and copper are complexing with each other. The presence of sulfur is important because it confirms the importance of the acid cleaning step in the copper surface preparation, likely being present as sulfate. Notably absent from the spectra is fluorine, which might be expected from the PAG. Tetrakis(pentafluorophenyl)boric acid (formed upon UV exposure of the PAG) degrades into volatile pentafluorobenzene, so after many months, no fluorine is present. It is possible that copper catalyzes this degradation. Copper is known to catalyze boration of enones[46] and esters,[47] which may indicate that boron is acting as the end-capping group rather than copper.

Techniques to prevent copper uptake into PPC as seen in Figs. 17 and 18 may be integrated synergistically into some process flows for fabricating electronic components. Thin-film dielectrics may be required with air cavities to provide confining stress and prevent surface diffusion of copper due to electromigration.[48] Plasma-enhanced chemical vapor deposition (PECVD) coating of SiO_2 or other thin-film dielectrics may be used to protect PPC from copper interaction. Similarly, metal barrier layers for subsequent process steps may be required on metal contacts to prevent formation of oxides or brittle intermetallics during processing.

In summary, the effect of trace amounts of copper ions on the thermal decomposition of PPC is described. It is shown that copper is taken up into solvent-cast, PAG-loaded PPC films. The incorporation of copper into the PPC film results in suppression of the thermal decomposition of the PPC, shifting the decomposition temperature to higher values by a significant amount. Three solvents were shown to be effective in the PPC temperature suppression process. One possible cause for the shift in temperature is by copper complexing the PPC ends and interrupting the normal product formation. The change in decomposition temperature has interesting practical effects for creating unique electronic structures including self-aligned air-gap structures on copper traces.

CONCLUSIONS

Self-patterned PPC can be employed to encapsulate copper lines on silicon and epoxy-fiberglass substrates by copper uptake into the PPC film to alter decomposition characteristics after UV exposure. Thermal stability increases for PPC films cast from GBL, TCE, and MeCl on copper substrates, allowing selective patterning around traces on a substrate using all three solvents. Patterning characteristics depend on copper line geometry and processing recipes. The self-patterning capability is valuable for creating air-cavity electrical interconnects with fewer process steps and at lower cost.

Although self-patterning of PPC is potentially advantageous for many applications, careful design is required to minimize process steps and barrier layers. Detailed analysis of diffusion rate, concentration profiles, patterning resolution and feature size, and temperature effects on film drying will be required for future process integration. Understanding of the mechanism and kinetics of copper uptake will also be required for process modeling.

Concentration is clearly important, as GBL films showed the highest thermal stability when the copper concentration was the highest. Measurements of lateral diffusion and TGA results emphasized the differences in decomposition rates due to copper concentration and availability. PPC films removed from copper also exhibit a light blue–green color not seen in other films, which may be indicative of elevated copper levels. For many consumer and optical applications, this shading may be an undesirable effect, but discoloration is acceptable in sacrificial applications for microelectronics as long as residue does not interfere with electrical performance.

ACKNOWLEDGEMENT

The authors acknowledge the financial support of the Interconnect Focus Center, one of the six research centers funded under the Focus Center Research Program, a Semiconductor Research Corporation program.

REFERENCES

1. D. Bhusari, H.A. Reed, M. Wedlake, A.M. Padovani, S.A. Bidstrup Allen, and P.A. Kohl, *J. MEMS* 10, 400 (2001).
2. B. Dang, P. Joseph, M. Bakir, T. Spencer, P. Kohl, and J. Meindl, *IEEE-IITC* (San Fransisco, CA, USA: IEEE, 2005).
3. H.A. Reed, C.E. White, V. Rao, S.A. Bidstrup Allen, C.L. Henderson, and P.A. Kohl, *J. Micromech. Microeng.* 11, 733 (2001).
4. S. Metz, S. Jiguet, A. Bertsch, and P. Renaud, *Lab Chip* 4, 114 (2004).
5. P.J. Joseph, P. Monajemi, F. Ayazi, and P.A. Kohl, *IEEE Trans. Adv. Packag.* 30, 19 (2007).

6. T.J. Spencer, P.J. Joseph, T.H. Kim, M. Swaminathan, and P.A. Kohl, *IEEE Trans. Microw. Theory Technol.* 55, 1919 (2007).
7. P.J. Jayachandran, H.A. Reed, H. Zhen, L.H. Rhodes, C.L. Henderson, S.A. Bidstrup Allen, and P.A. Kohl, *J. MEMS* 12, 147 (2003).
8. M.G. Cupta, P.J. Joseph, and P.A. Kohl, *J. Appl. Polym. Sci.* 105, 2655 (2007).
9. T.J. Spencer and P.A. Kohl, *Poly. Deg. Stab.* (in press, 2010).
10. S. Chen, Z. Xiao, and M. Ma, *J. Appl. Polym. Sci.* 107, 3871 (2008).
11. L.C. Du, Y.Z. Meng, S.J. Wang, and S.C. Tjong, *J. Appl. Polym. Sci.* 92, 1840 (2004).
12. B. Liu, X. Zhao, X. Wang, and F. Wang, *J. Appl. Polym. Sci.* 90, 947 (2003).
13. G.A. Luinstra, *Polym. Rev.* 48, 192 (2008).
14. G.A. Luinstra, G.R. Haas, F. Molnar, V. Bernhart, R. Eberhart, and B. Rieger, *Chem. Eur. J.* 11, 6298 (2005).
15. G.A. Luinstra and F. Molnar, *Macromol. Symp.* 259, 203 (2007).
16. Y. Niu, W. Zhang, H. Li, X. Chen, J. Sun, X. Zhuang, and X. Jing, *Polymer* 50, 441 (2009).
17. Y. Qin, X. Wang, S. Zhang, X. Zhao, and F. Wang, *J. Appl. Polym. Sci.: A: Chem.* 46, 5959 (2008).
18. Y. Tao, X. Wang, X. Chen, X. Zhao, and F. Wang, *J. Appl. Polym. Sci.: A: Chem.* 46, 4451 (2008).
19. B. Li, G.P. Wu, W.M. Ren, Y.M. Wang, D.Y. Rao, and X.B. Lu, *J. Appl. Polym. Sci.: A: Chem.* 46, 6102 (2008).
20. X.H. Li, Y.Z. Meng, Q. Zhu, and S.C. Tjong, *Polym. Degrad. Stab.* 81, 157 (2003).
21. S. Peng, Y. An, C. Chen, B. Fei, Y. Zhuang, and L. Dong, *Polym. Degrad. Stab.* 80, 141 (2003).
22. M. Cupta (Ph.D. Thesis, Georgia Tech, 2005), p. 137.
23. Q. Zhu, Y.Z. Meng, S.C. Tjong, X.S. Zhao, and Y.L. Chen, *Polym. Int.* 51, 1079 (2002).
24. Y.S. Qin, W.M. Qing, H.W. Xian, J.Z. Sun, X.J. Zhao, and F.S. Wang, *Polym. Degrad. Stab.* 92, 1942 (2007).
25. Y. Tao, X. Wang, X. Zhao, J. Li, and F. Wang, *J Appl. Polym. Sci.: A: Chem.* 44, 5329 (2006).
26. L.J. Gao, F.G. Du, M. Xiao, S.J. Wang, and Y.Z. Meng, *J. Appl. Polym. Sci.* 108, 3626 (2008).
27. L.J. Gao, M. Xiao, S.J. Wang, and Y.Z. Meng, *J Appl. Polym. Sci.: B: Polym. Phys.* 108, 1037 (2008).
28. P.F. Song, M. Xiao, F.G. Du, S.J. Wang, L.Q. Gan, G.Q. Liu, and Y.Z. Meng, *J. Appl. Polym. Sci.* 109, 4121 (2008).
29. L. Du, B. Qu, Y. Meng, and Q. Zhu, *Compos. Sci. Technol.* 66, 913 (2006).
30. T. Yu, Z. Yong, K. Liu, Y. Zhao, E. Chen, F. Wang, and D. Wang, *Polym. Degrad. Stab.* 94, 253 (2009).
31. T. Yu, Y. Zhou, Y. Zhao, K. Liu, E. Chen, D.Y. Wang, and F. Wang, *Macromolecules* 41, 3175 (2008).
32. Z. Zhang, J. Lee, S. Lee, S. Heo, and C.U. Pittman Jr., *Polymer* 49, 2947 (2008).
33. Z. Zhang, Z. Mo, H. Zhang, Y. Zhang, T. Na, Y. An, X. Wang, and X. Zhao, *J. Polym. Sci. B: Polym. Chem.* 40, 1957 (2002).
34. Z. Zhang, Q. Shi, J. Peng, J. Song, Q. Chen, J. Yang, Y. Gong, R. Ji, X. He, and J.H. Lee, *Polymer* 47, 8548 (2006).
35. Z. Zhang, H. Zhang, Q. Zhang, Q. Zhou, H. Zhang, Z. Mo, X. Zhao, and X. Wang, *J. Appl. Polym. Sci.* 100, 584 (2006).
36. X. Shi and Z. Gan, *Eur. Polym. J.* 43, 4852 (2007).
37. R.E. Zacharia, S.L. Simon, E.J. Beckman, and R.M. Enick, *Polym. Degrad. Stab.* 63, 85 (1999).
38. M.S. Wu, P.C.J. Chiang, J.C. Lin, and J.T. Lee, *Electrochim. Acta* 49, 4379 (2004).
39. C.E. Anson, L. Ponikiewski, and A. Rothenberger, *Zeitschrift für anorganische und allgemeine Chemie* 632, 2402 (2006).
40. A.P. Purdy, D. Godbey, and L. Buckley, *Thin Solid Films* 308-309, 486 (1997).
41. J.V. Crivello, T.P. Lockhart, and J.L. Lee, *J. Polym. Sci.: A: Polym. Chem.* 21, 97 (1983).
42. L.T. Guan, F.G. Du, G.Z. Wang, Y.K. Chen, M. Xiao, S.J. Wang, and Y.Z. Meng, *J. Polym. Res.* 14, 245 (2007).
43. L.T. Guan, M. Xiao, and Y.Z. Meng, *Polym. Eng. Sci.* 46, 153 (2006).
44. X.H. Li, S.C. Tjong, Y.Z. Meng, and Q. Zhu, *J. Polym. Sci.: B: Polym. Phys.* 41, 1806 (2003).
45. X. Ma, P.R. Chang, J. Yu, and N. Wang, *Carbohydr. Polym.* 71, 229 (2008).
46. I.H. Chen, L. Yin, W. Itano, M. Kanai, and M. Shibasaki, *J. Am. Chem. Soc.* 131, 11664 (2009).
47. V. Lillo, A. Prieto, A. Bonet, M.M. Di-Requejo, J. Ramirez, P.J. Pérez, and E. Fernández, *Organometallics* 28, 659 (2009).
48. Z.S. Choi, R. Monig, and C.V. Thompson, *J. Appl. Phys.* 102, 083509-1 (2007).